

Preparation and Structure of Aluminosilicate Aerogels

F. Chaput,[†] A. Lecomte,[‡] A. Dauger,[‡] and J. P. Boilot*[†]

Groupe de Chimie du Solide, Laboratoire de Physique de la Matière Condensée, Ecole Polytechnique, 91128 Palaiseau Cédex, France, and Ecole Nationale Supérieure de Céramique Industrielle, 87065 Limoges Cédex, France

Received August 9, 1988

Monolithic aluminosilicate aerogels have been prepared from the $(\text{BuO})_2\text{Al-O-Si}(\text{OEt})_3$ double precursor. Small-angle X-ray scattering indicates that aluminosilicate aerogel structures can be represented by primary units that stick together into mass-fractal clusters ($D = 1.80-1.85$) by a mechanism of cluster-cluster aggregation. Self-similarity is displayed in the aluminosilicate aerogels in a large range of densities (from 50 to 250 kg/m^3).

Introduction

Aerogels are low-density porous materials made by supercritical drying of gels. Silica aerogels were first produced by Kistler¹ in 1932 and were characterized as an open, cross-linked silica structure with a high fraction of voids with extremely fine pore sizes.² They typically exhibit very high surface area, low refractive index, low thermal conductivity, low sound velocity, and visible transparency. This unusual combination of properties makes the aerogel a unique material suited for a diverse array of applications: insulating transparent glazings³ (windows, solar collector covers, etc.); Cherenkov radiation detectors;^{4,5} catalyst supports;⁶ filters, membranes; acoustic delay lines; oxide ceramic precursors.⁷ Comparatively, very little is known about aerogel synthesis in more complex multicomponent system.^{8,9}

In the H_2O , HO^iPr , $(\text{BuO})_2\text{Al-O-Si}(\text{OEt})_3$ ternary phase diagram, various factors affecting the gelation process (nature of the solvent, pH, temperature, concentration) have been investigated to find appropriate experimental conditions for making aluminosilicate alcogels.¹⁰ In fact, we have shown that optically clear alcogels can be prepared within a large range of oxide concentrations. The gelation time is mainly governed by the initial water concentration, showing that the hydrolysis of Si-OR groups is the rate-determining process for the gelation. Nuclear magnetic resonance,¹¹ small-angle X-ray scattering,¹² and small-angle neutron scattering¹³ studies of the gelation from the double precursor $(\text{BuO})_2\text{Al-O-Si}(\text{OEt})_3$ have shown that, in the first steps, a rapid formation of primary polymeric particles takes place by condensation between Al-OH groups. These units formed of Al-O-Al linkages are then agglomerated by a cluster aggregation process chemically limited by the hydrolysis of the Si-OR groups.

In this paper, we report the preparation of monolithic aluminosilicate aerogels with different densities and structural results obtained by small-angle X-ray scattering (SAXS).

Experimental Section

Transparent alcogels have been prepared in the $\text{H}_2\text{O}/\text{HO}^i\text{Pr}/(\text{BuO})_2\text{Al-O-Si}(\text{OEt})_3$ ternary phase system. A mixture of isopropyl alcohol and water containing 6.3×10^{-4} mol L^{-1} of a strong acid (HCl) was slowly poured into a mixture of precursor and isopropyl alcohol. The initial composition, noted 1:4:2, corresponds to one volume of water, four of solvent, and two of precursor. Other compositions were obtained by dilution with 2-propanol. Samples were kept in sealed glass containers at 25 °C, and the gel time was defined by observing the stiffness after tilting the container. For all of the samples, no significant change

of volume was noted at the gel point.

The alcogel structure typically contains more than 90% by volume fine pores confining alcohol. To make aluminosilicate alcogels useful for applications, the liquid solvent filling the void space must be removed. During conventional drying, the interfacial forces generated in the small pores at the liquid-gas boundary are very high. To prevent damage to the gel structure caused by these interfacial forces, the alcohol removal must be done under supercritical conditions, so that there is no distinction between gas and liquid, and therefore these forces are eliminated.

For the supercritical evacuation of the solvent, the gels were introduced into an autoclave (Figure 1) into which a volume of 2-propanol was added to attain a pressure higher than the critical pressure at critical temperature. The temperature was increased to 245 °C, and the corresponding pressure is approximately 65 bars (for the pure 2-propanol, the temperature and the pressure corresponding to the critical point are respectively 235 °C and 48 bars). The temperature was kept constant, and a slow evacuation of the solvent was performed (Figure 2). Supercritical drying of aluminosilicate alcogels leads to aerogels that exhibit different densities. The apparent density (ρ) measured by Hg volumetry varied from 50 to 250 kg/m^3 , and transparency to visible light is observed for samples in the density range from 100 to 250 kg/m^3 .

Small-angle X-ray scattering (SAXS) data from aluminosilicate aerogels were recorded with a slit type camera (Cu $K\alpha$ wavelength). The sample-to-detector distance was 500 mm, and the scattered intensity was counted with a linear position-sensitive counter. The scattering vector $K = (4\pi \sin \theta)/\lambda$, where θ is the Bragg angle, ranges from 6×10^{-3} to 2×10^{-1} Å^{-1} . Experimental results were corrected for parasitic scattering and normalized to equivalent sample thickness, incident intensity, and counter efficiency. Aerogel slices of about 2 mm in thickness and 10 mm in diameter were used.

Scattering in the Guinier region (low angles) depends on the characteristic dimension R of the scattering entities and from the

(1) Kistler, S. S. *J. Phys. Chem.* **1932**, *36*, 52.

(2) Fricke, J. *J. Non-Cryst. Solids* **1987**, *95*, 1135.

(3) Tewari, P. H.; Hunt, A. J.; Loftus, K. D. *Aerogels*; Springer Progress in Physics; Springer: Heidelberg, 1986; Vol 6, p 31.

(4) Cantin, M.; Cassee, M.; Koch, L.; Jouan, R.; Mestreau, P.; Roussel, D. *Nucl. Instrum. Methods* **1974**, *118*, 177.

(5) Bourdinard, M.; Close, J. B.; Thevenin, J. C. *Nucl. Instrum. Methods* **1976**, *136*, 99.

(6) Reis, H. *Adv. Catal.* **1952**, *4*, 99.

(7) Chaput, F.; Boilot, J. P.; Papiernick, R.; Hubert-Pfalzgraf, L. G.; Lejeune, M. *J. Am. Ceram. Soc.*, in press.

(8) Woignier, T.; Phalipou, J.; Zarzycki, J. *J. Non-Cryst. Solids* **1984**, *63*, 117.

(9) Brinker, C. J.; Ward, K. J.; Keefer, K. D.; Holupka, E.; Bray, P. J.; Pearson, R. K. *Aerogels*; Springer Progress in Physics; Springer: Heidelberg, 1986; Vol. 6, p 57.

(10) Pouxviel, J. C.; Boilot, J. P. *J. Mater. Sci.*, in press.

(11) Pouxviel, J. C.; Boilot, J. P.; Dauger, A.; Huber, L. *Better Ceramics Through Chemistry II. MRS Proc.* **1986**, *73*, 269.

(12) Pouxviel, J. C.; Boilot, J. P.; Lecomte, A.; Dauger, A. *J. Phys. (Paris)* **1987**, *48*, 921.

(13) Pouxviel, J. C.; Boilot, J. P.; Dauger, A.; Wright, A. *J. Non-Cryst. Solids* **1988**, *103*, 331; *Better Ceramics Through Chemistry III. MRS Proc.* **1988**, *121*, 121.

[†]Groupe de Chimie du Solide.

[‡]Ecole Nationale Supérieure de Céramique Industrielle.

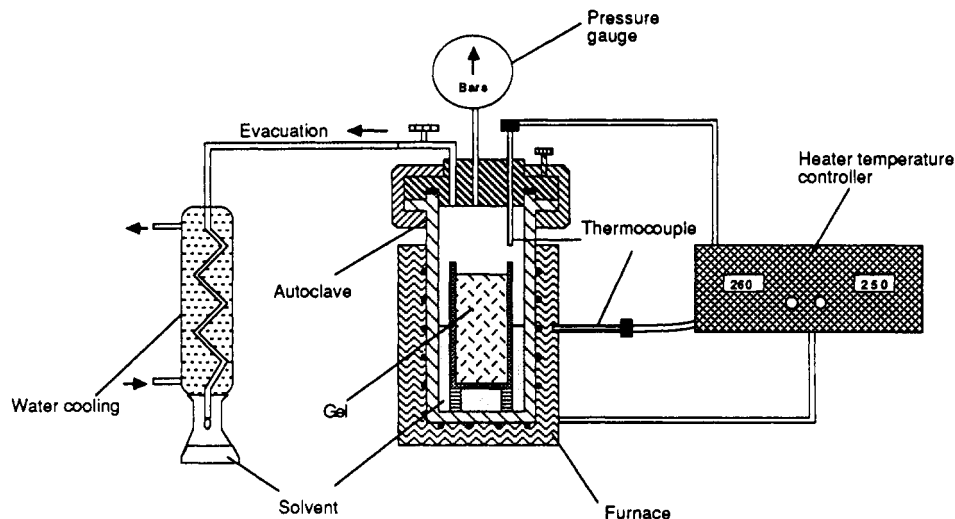


Figure 1. Autoclave equipment.

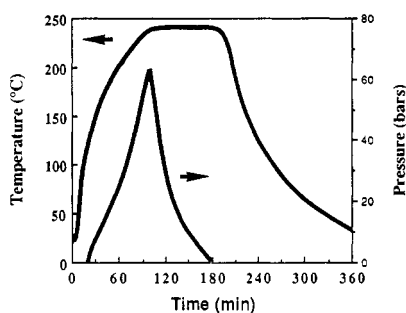


Figure 2. Time dependence of the temperature and of the pressure in the autoclave during the preparation of the aluminosilicate aerogels.

initial decay of the scattered intensity $I(K)$. One can deduce the electronic radius of gyration, R_g , using the following formula:¹⁴

$$I(K) = n_p^2 N (1 - K^2 R_g^2 / 3) \quad (1)$$

($R_g = (3/5)^{1/2} R$ for spherical particles) where K is the scattering wave vector, N is the number of scattering particles, and n_p is the number of electrons in each particle ($n_p = \rho_p V_p$, where ρ_p is the electronic density of particles of volume V_p).

Scattering in the Porod region defined as $KR \gg 1 \gg Ka$, where the monomer size is a , depends on the geometric structure of the scattering entities.¹⁴ The scattered intensity decays as the power law $I(K) \sim K^{-x}$, and therefore, in a log-log plot of $I(K)$ versus the scattering vector, the slope is sensitive to the geometry of the scatterers. For polymer-like structures¹⁵ (mass-fractal objects) the classic power law exponent x observed in the Porod regime is the fractal dimension D , which relates the size R of the object to its mass, $M \sim R^D$.

Results

For all the samples, two power law regimes are seen in the Porod range with slopes of -1.85 and -4 (Figure 3). The crossover is approximately the same for all the samples and occurs at about $K = 7.5 \times 10^{-2} \text{ \AA}^{-1}$, corresponding to a length of 13 \AA . With a fractal model to interpret the scattering data, the picture that emerges is a scattering from a smooth surface of homogeneous particles at short length scales ($< 13 \text{ \AA}$) and scattering from a mass fractal of dimension 1.85 at larger scales. Therefore, as observed for silica aerogels,¹⁶ the SAXS study indicates that the

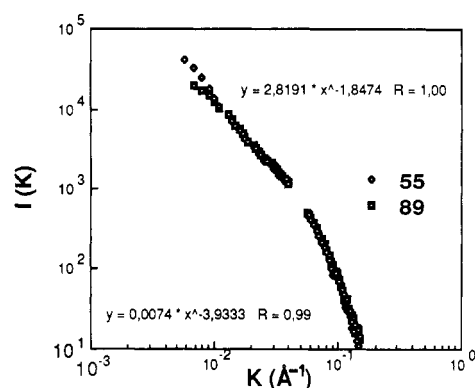


Figure 3. Porod plots for aluminosilicate aerogels showing two power law regimes with slopes of -1.85 and -4 . The crossover approximately occurs at $K = 7.5 \times 10^{-2} \text{ \AA}^{-1}$. The curves are labeled with ρ in kg/m^3 . The curve corresponding to the sample with $\rho = 55 \text{ kg/m}^3$ has been used for the fit.

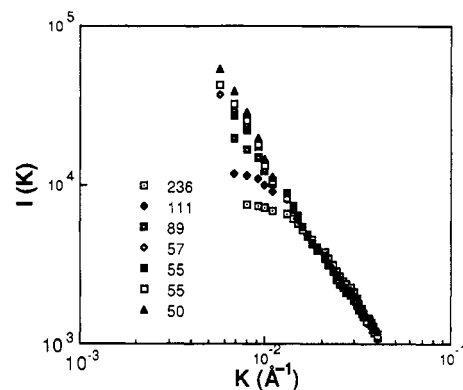


Figure 4. Scattered intensities at low K and in the intermediate K range for different aluminosilicate aerogel samples (the curves are labeled with ρ in kg/m^3) showing that each sample has about the same fractal dimension and that the fractal range decreases in size with increasing density.

aerogel structure can be represented by a two-level structure: It consists of primary dense particles (density ρ_a and size a) attached into mass-fractal clusters by a mechanism of cluster-cluster aggregation.

Figure 4 shows scattered intensities at low K and in the intermediary K range for six samples. The data were normalized to equivalent sample thickness but not shifted

(14) Guinier, A.; Fournet, G. *Small Angle Scattering of X-rays*; John Wiley and Sons: New York, 1955.

(15) Schaefer, D. W.; Keefer, K. D. *Phys. Rev. Lett.* 1984, 53, 1383. *Fractals in Physics*; Pietronero, L., Tosatti, E., Eds.; Elsevier Science Publishers: Amsterdam, 1986; p 39.

(16) Schaefer, D. W.; Keefer, K. D. *Phys. Rev. Lett.* 1986, 56, 2199.

with respect to each other. For high-density samples a third regime exists at small K consistent with uniform nonfractal long-range structure, corresponding to a decrease of the fractal range (R (Å) in size) with increasing density. Moreover, it seems that each sample has the same fractal dimension and that, in the fractal range, the different samples cannot be distinguished. This indicates, as previously displayed in the silica system,¹⁷ the existence of mutual self-similarity within a large range of densities. In fact, a slight deviation from a power law is observed, in a small K regime, for low-density samples which exhibit concave upward scattering curves probably due to interference effects.¹³ Therefore, the data are not mutually self-similar on large length scales.

From the initial decay of the intensity in the Guinier region, we have deduced the electronic radius of gyration R_g . Obviously, it is clear from the curves in Figure 4 that the data for densities below 89 kg/m³ cannot be accurately analyzed to extract the radius of gyration or the intensity at $K = 0$. However, if we use the Guinier approximation for only the three more dense samples and assume, as observed in the silica system,¹⁷ that the function relating the extension of the fractal domain to the density is the same for all the samples, we find $R_g = 18.7\rho^{-0.84}$. Using the mass-fractal law $\rho_p/\rho_a = (R/a)^{D-3}$, taking the same description for primary units, and considering as equal the density of the fractal particles and the average density of the sample ($\rho_p = \rho$), one finds $D = 1.81$, a value close to that determined from Figure 3. Moreover, the prefactor value (18.7) is consistent with the existence of spherical primary units (13 Å in size) of density 2.1 g/cm³, which is relatively close to that (2.5 g/cm³) of the usual aluminosilicate glass with the same composition (Al/Si molar ratio = 1).¹⁸

Conclusions

Aluminosilicate alcogels can be prepared from the (BuO)₂Al–O–Si(OEt)₃ complex precursor in a large range of oxide concentrations. Supercritical drying of aluminosilicate alcogels in an autoclave system (65 bars, 245 °C) leads to aluminosilicate aerogels that exhibit transparency to visible light in the density range from 100 to 250 kg/m³.

In spite of the small range size explored, the SAXS study indicates that the aerogel structure can be described by a two-level structure: It consists of primary units, homogeneous dense particles (density 2.1 g/cm³ and 13 Å in size), that are attached into mass fractal clusters. The

fractal dimension is in agreement with a cluster–cluster growth mechanism.

As previously displayed in the silica system, aluminosilicate aerogels seem to be mutually self-similar within a large range of densities (from 50 to 250 kg/m³).

Concerning the aggregation process, there are two limiting models. The first, called cluster–cluster diffusion-limited aggregation, has been extensively studied by computer simulations.^{19,20} In this model, clusters stick together after diffusing in a purely random-walk fashion in empty space. The result of this process is an open highly ramified object with a fractal dimension of the clusters of 1.78. In fact, it is probably more realistic to assume that the clusters do not stick on every contact. Simulations of diffusion-limited aggregation with very low sticking probability²¹ yield a fractal dimension of 2–2.1. This type of aggregation is a reaction-limited process and is called the reaction-limited cluster aggregation (RCLA). For instance, aggregation in the silica¹⁵ system leads to a fractal dimension of 2 consistent with the RCLA model. In contrast, we only found 1.80–1.85 for the Al–O–Si aerogel. Moreover, a close value (1.8–1.9) has been previously observed for different Al–O–Si alcogels,^{12,13,22} showing that the change of the aggregation conditions does not influence the fractal dimension. This special behavior compared to pure silica may be due to the large Si(OR)₃ unhydrolyzed groups, detected by ²⁹Si NMR, which reduce the degree of branching and probably lead to orientational effects for condensation reactions.

Concerning the structure of the primary units, a compact nature is observed for aerogels (slope of –4). However, the fact that the aluminum part of the (BuO)₂Al–O–Si(OEt)₃ monomer hydrolyzes more rapidly is not sufficient to completely explain this structure because the scattering curves of the corresponding alcogel¹² show limiting high K slopes of only –2.6. Nevertheless, it is clear that for alcogels, the density of primary particles depends on the hydrolytic conditions and on the reactivity of the precursor. For instance, scattering curves of other aluminosilicate alcogels, prepared by slow hydrolysis in air moisture of the (iPrO)₂Al–O–SiMe₃ aluminosiloxane precursor exhibit a limiting high K slope of –1.2, corresponding to a very ramified structure at short length scale.²² In these hydrolytic conditions, the units grow from the condensation between partially hydrolyzed aluminum groups. In all cases, it seems that the supercritical drying turns polymeric units of the alcogel into compact particles.

(17) Vacher, R.; Woignier, T.; Pelous, J.; Courtens, E. *Phys. Rev.* **1988**, *B37*, 6500.

(18) Jantzen, C. M.; Schwahn, D.; Schelten, J.; Herman, H. *Phys. Chem. Glasses* **1981**, *22*, 139.

(19) Meakin, P. *Phys. Rev. Lett.* **1983**, *51*, 1119.

(20) Kolb, M.; Botet, R.; Jullien, R. *Phys. Rev. Lett.* **1983**, *51*, 1123.

(21) Kolb, M.; Botet, R.; Jullien, R. *J. Phys. Lett.* **1984**, *45*, 211.

(22) Pouxviel, J. C.; Boilot, J. P.; Poncelet, O.; Hubert-Pfalzgraf, L. G.; Lecomte, A.; Dager, A.; Beloeil, J. C. *J. Non-Cryst. Solids* **1987**, *93*, 277.